Actin in the Photoreceptor Connecting Cilium: Immunocytochemical Localization to the Site of Outer Segment Disk Formation

MICHAEL H. CHAITIN, BARBARA G. SCHNEIDER, MICHAEL O. HALL,* and DAVID S. PAPERMASTER

*Department of Pathology, Yale Medical School, New Haven, Connecticut 06510; Veterans Administration Medical Center, West Haven, Connecticut 06516; and *Jules Stein Eye Institute, University of California School of Medicine, Los Angeles 90024. Dr. Chaitin's present address is the Jules Stein Eye Institute.*

ABSTRACT Actin has been localized in *Rana pipiens* retinas that were fixed and embedded in aldehyde cross-linked BSA. Thin sections were reacted sequentially with (*a*) affinity-purified antiactin antibodies induced in rabbits; (*b*) biotinyl-sheep anti-rabbit antibodies; and (c) avidin-ferritin conjugates. As expected, antiactin labeling density was high in the apical pigment epithelial cell processes and in the calycal processes of photoreceptors. Actin was also localized in a new site. The connecting cilium that joins the inner and outer segments of both rods and cones was heavily labeled by antiactin at its outer segment (OS), or distal, end. In this region of the cilium, the plasma membrane evaginates to form new OS disks and these basal disks were labeled in some instances. Below the new disks in rods, the cytoplasm of liplike expansions of the distal cilium was also heavily labeled. The plasma membrane and interior of the connecting cilium and the remainder of the OS were unlabeled. These findings suggest that actin may participate in the vectorial transport of opsin and other intrinsic membrane proteins that are incorporated into newly forming OS disks. The results also implicate actin in the membrane expansion involved with OS disk formation.

Retinal rod and cone photoreceptors are highly polarized cells in which the light sensitive outer segment (OS) is connected to the remainder of the cell by a nonmotile cilium (Fig. 1). The OS of rods is comprised of a plasma membrane enclosed stack of hundreds of membranous disks that contain the visual pigment rhodopsin as an integral membrane protein. Opsin, the apoprotein of rhodopsin, is synthesized in the inner segment of the cell (1–4) and is membrane bound in vesicles or cisternae as it is vectorially transported to the base of the connecting cilium (*CC*; 3, 5). It has been suggested that these vesicles fuse with the apical plasma membrane of the rod inner segment (5, 6), possibly in a recently described surface domain known as the periciliary ridge complex (*PRC*; 7) (Fig. 2). Opsin may migrate from the *PRC* along the *CC* plasma membrane to its site of incorporation into *OS* disks. A similar pathway is postulated for a high molecular weight intrinsic membrane protein recently localized to the margins and incisures of OS disks (8–10).

The OS undergoes a unique form of membrane renewal. At the base of the OS the CC plasma membrane evaginates to form flattened lamellae that expand in size to the full diameter of the OS (7, 11) (Fig. 2). In cones these lamellae remain open to the extracellular space, whereas in rods they separate from the OS plasma membrane and become isolated disks. In rods, as newer disks are formed the older ones are gradually displaced toward the apex of the OS where they are intermittently shed in packets that are ingested by adjacent pigment epithelial (*PE*) cells (12, 13) (Fig. 1). Rods shed the major portion of their OS disks following light onset (14, 15). Cones also shed their OS material but the timing of this event varies in different species (16, 17).

The PE cells extend long, thin, cytoplasmic processes that interdigitate with and ensheath the OS (Fig. 1). These processes play a role in the phagocytosis of shed OS material and contain parallel arrays or bundles of axially oriented actin filaments (18–20). Actin filament bundles are also observed in photoreceptor calycal processes (21). These are microvillus-like projections that arise from the inner segment and extend alongside the basal OS (Figs. 1 and 2).

A relatively constant OS length is maintained by a balance

THE JOURNAL OF CELL BIOLOGY · VOLUME 99 JULY 1984 239–247

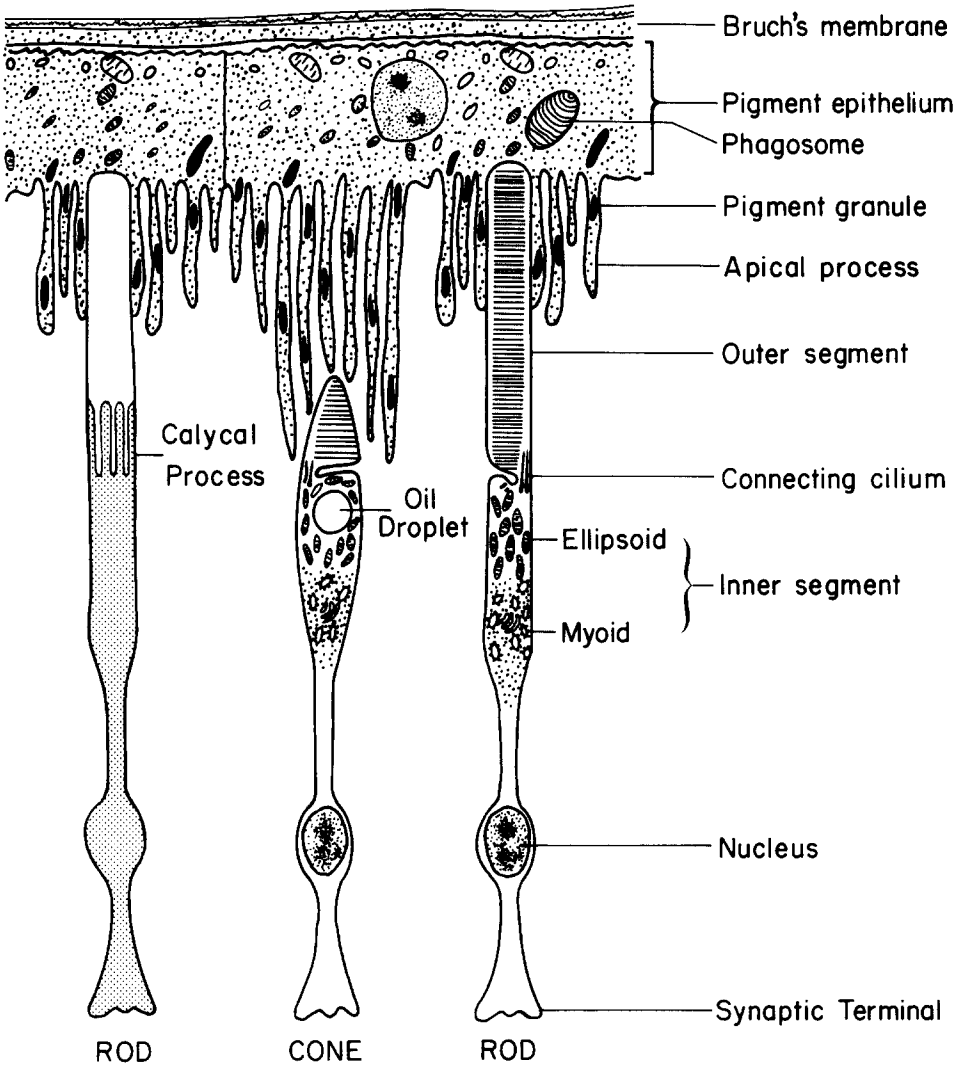

FIGURE 1 Diagram showing the pigment epithelium and adjacent photoreceptors. The two photoreceptors on the right represent internal views of a rod and a cone. Note the subdivisions of these cells. The photoreceptor on the left is an external view of a rod showing the many calycal processes that project from the inner segment and extend alongside the basal outer segment. Calycal processes are found in both rods and cones. Apical processes of the pigment epithelium interdigitate with and surround the photoreceptor outer segments. Phagosomes are shed packets of outer segment disks that have been ingested by the pigment epithelium.

between the processes of disk formation and disk shedding. Although much information has been gathered about the effects of light and temperature on these two processes (for review see reference 22), the molecular events that underlie OS renewal are still not understood. A contractile mechanism may mediate the vectorial transport of opsin to the OS, as well as the membrane expansion involved in OS disk formation. To examine this hypothesis, we conducted an immunocytochemical study in which thin sections of albumin embedded retinas were labeled with antiactin antibodies. As expected, heavy labeling of actin occurred in the PE processes and calycal processes. The presence of actin was also demonstrated in a new site. A dense, localized concentration of actin was observed in the distal portion of the CC at the site of OS disk formation in both rod and cone photoreceptors.

MATERIALS AND METHODS

Animals: Frogs (*Rana pipiens* adults) were kept on a 12-h light/12-h dark cycle and sacrificed at various times of the day and night. For all samples taken at night, the frogs were killed and the eyes dissected under dim red light. One of the frogs was exposed to the natural midautumn diurnal cycle and was killed 1 h after the onset of light in the morning.

Tissue Processing: Animals were decapitated, the eyes removed, and the eyecups fixed at room temperature either in 2% paraformaldehyde, 2.5% glutaraldehyde, 0.1 M sodium cacodylate, pH 7.4, for 2 or 3.5 h, or in 1.2% glutaraldehyde, 0.15 M sodium phosphate, pH 7.0 for 2 h. The eyecups were rinsed in cacodylate or phosphate buffer, cut into strips and embedded in formaldehyde- or glutaraldehyde-crosslinked BSA (Armour Reheis, fraction V) as described previously (4, 23–25).

Preparation of Antibodies: Antiactin antibodies were induced in rabbits using actin purified from chicken gizzards (26). The immunization schedule followed was that described by Jockusch et al. (27) and the antiactin was purified from immune serum using affinity chromatography. For this study the actin used to prepare an actin-Sepharose column was purified as follows. An acetone powder was prepared from fresh chicken gizzards as outlined by Herman and Pollard (28). Actin was extracted following the method of Spudich and Watt (29), with modifications (26). The depolymerized actin was passed over a Sephadex G-150 column equilibrated in the actin depolymerizing buffer. The peak actin containing fractions were pooled, concentrated, and bound to CNBr-activated Sepharose 4B (Pharmacia Fine Chemicals, Inc.) as previously described (26, 27).

Immune serum was mixed with the actin-Sepharose beads. The bound antiactin antibodies were eluted with 4 M $MgCl_2$ and dialyzed against borate buffer, pH 8.0 containing 0.02% sodium azide. The antiactin antibodies were concentrated to 0.15 mg/ml and BSA (CalBiochem-Behring Corp., San Diego, CA, fraction V) was added to 1%. For immunocytochemistry, antiactin was used at this concentration or diluted to a concentration of 0.10 or 0.05 mg/ml.

Biotinyl IgG or $F(ab')_2$ of sheep anti-rabbit $F(ab')_2$ was prepared by reaction with biotin *N*-hydroxysuccinimide ester (30). Six times crystallized horse spleen ferritin (Miles Laboratories, Inc., Elkhart, IN), with no further purification, was conjugated to avidin (Sigma Chemical Co., St. Louis, MO, # A-9390) following the glutaraldehyde conjugation method (31).

Retinal thin sections were collected on carbon and formvar coated copper grids and were stored dry until use. At room temperature, grids were transferred sequentially to drops of 0.1 M Tris-Cl, pH 7.4 (5 min); 4% BSA in Tris-Cl (10

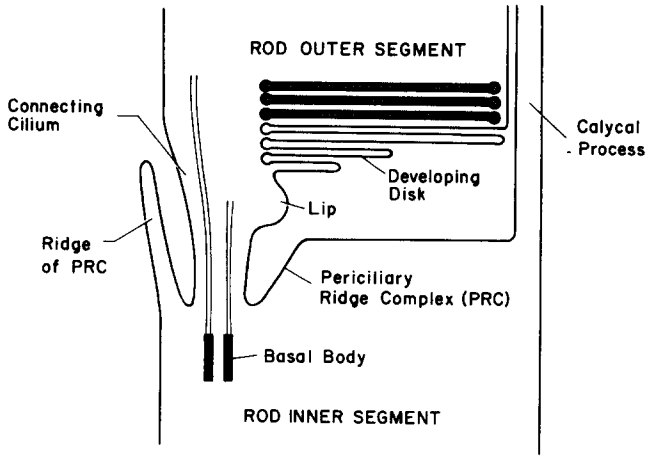

FIGURE 2 Diagram showing the connecting cilium and junctional region between the inner and outer segments of a rod. Outer segment disks develop from evaginations of the cilium plasma membrane. In rods these lamellae expand to the full diameter of the outer segment and then separate from the plasma membrane to form isolated disks. During this renewal process, what had been the space between two expanding lamellae becomes the intradiscal space of an isolated disk. A liplike structure protrudes from the distal cilium just below the developing disks. Note the difference between a calycal process and the lateral inner segment process, which is a ridge of the periciliary ridge complex.

min); 0.02 M glycine in Tris-Cl (15 min); antiactin antibodies (15 min); Tris-Cl (6 × 1 min); 0.1 mg/ml biotinyl sheep anti-rabbit IgG (15 min); Tris-Cl (6 × 1 min); avidin-ferritin, 0.06 mg/ml in ferritin (30 min), or 0.03 mg/ml (40 min); Tris-Cl (6 × 1 min); 0.1 M sodium phosphate, pH 7.4 (6 × 1 min); 2% glutaraldehyde in phosphate buffer (20 min); water (8 × 1 min); bismuth subnitrate (45 min; reference 32); water rinse; 10% uranyl acetate in 25% ethanol (15 min); water rinse. For a detailed review of the albumin embedding technique used for immunocytochemistry, see Schneider and Papermaster (25).

In control experiments nonimmune rabbit IgG was substituted for the antiactin in the labeling procedure. All tissue sections were examined in a Philips 300 electron microscope operated at 60 KeV.

Morphometric Analysis: For the quantitation of antiactin antibody labeling, micrographs were taken at a magnification of ×17,000 of different areas of photoreceptor and PE cells. Contact positives on the same film were made and viewed on a Bellco Plaque Viewer (Bellco Glass, Inc., Vineland, NJ). A template consisting of a double lattice grid system was placed on the screen. Ferritin grains per square were counted over areas of interest and the mean grain counts per square micron (± SE) were calculated as previously described (25).

RESULTS

The affinity-purified antiactin antibodies had previously been used in an immunofluorescence study with cultured rat PE cells (26). The antiactin antibodies labeled stress fibers in these cultured cells, as well as actin containing feltworks associated with newly phagocytized rod outer segment (ROS) fragments. Similar patterns of actin distribution have been reported for other types of cultured cells. In the present study

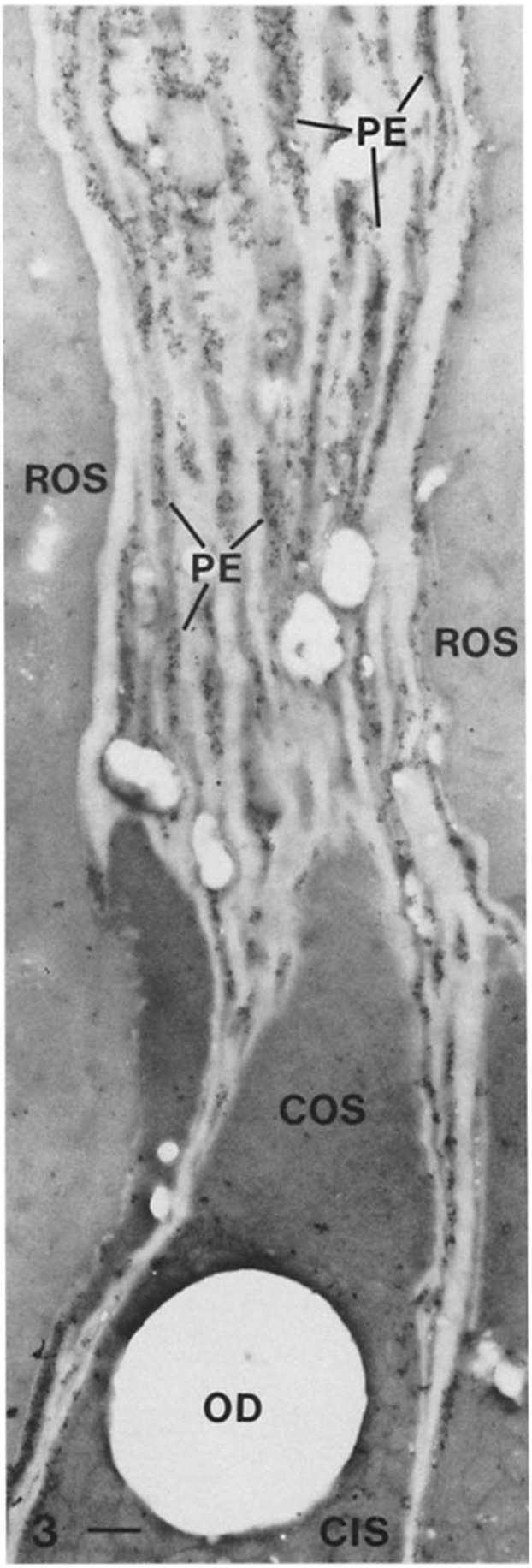

FIGURE 3 Thin section of an albumin embedded frog retina labeled with antiactin antibodies. Bound antibody is revealed by sequential reaction with biotinyl antiantibody and avidin-ferritin conjugates. Antiactin heavily labels actin in pigment epithelial processes (*PE*) which extend toward and surround a cone outer segment (*COS*) and two adjacent rod outer segments (*ROS*). *ROS* and *COS* are unlabeled. *CIS*, cone inner segment; *OD*, oil droplet. Bar 0.5 um; × 16,324.

we used these antiactin antibodies to label actin in thin sections of albumin-embedded frog retinas. The antiactin heavily labeled PE processes that surround ROS and cone outer segments (COS) (Fig. 3). Label was also concentrated in the apical region of the PE adjacent to the ROS tips (Fig. 4). Newly formed phagosomes that contained shed ROS material were surrounded by actin in the apical PE, whereas phagosomes that had moved deeper into the PE cell body were no longer surrounded by actin (Fig. 4). Antiactin did not specifically label either ROS or COS (Figs. 3 and 4, Table I).

Antiactin also heavily labeled photoreceptor calycal processes which are long tapered projections arising from the inner segments and extending alongside the basal portions of the OS (Fig. 5*a*). The label extended from the calycal processes deep into the inner segment, subjacent to the plasma membrane. In cross-sectioned rods, labeled calycal processes were observed to lie along the indentations of the ROS (Fig. 5*b*). Labeled actin bundles of the calycal processes continued into the ellipsoid (mitochondria rich region) of the inner segment (Fig. 5*c*). In the lower ellipsoid, near the junction with the myoid, these bundles separated into a more uniform distribution of actin lying just beneath the plasma membrane (Fig. 5*d*). The inner segment of frog photoreceptors was not specifically labeled aside from the actin bundles which extended from the calycal processes (Fig. 5, Table I).

Actin was also localized to a new site in rods and cones. Antiactin label was heavily concentrated in the distal portion of the rod CC and in the interior of a lip-like structure that protrudes from the rod CC just below the basal ROS disks (Fig. 6*a*). In this region the CC plasma membrane evaginates to form new ROS disks. The plasma membrane of the lip was unlabeled. When the plane of section was rotated such that the CC appeared to be in the middle of the cell, more than one labeled lip could be viewed (Fig. 6, *b* and *c*). In cones, antiactin was also concentrated in the distal portion of the CC (Fig. 6*d*) at the site where new COS disks are formed, however lip-like expansions of the CC were not observed. In cross-section, the proximal portion of the CC below the actin-rich domain was observed to be free of label (Fig. 7). Antiactin label occasionally extended from the distal portion of the CC along the length of the basal OS disks in both rods and cones (Fig. 8). The OS itself was otherwise unlabeled. In both rods and cones, antiactin did not specifically label the interior of the CC or its plasma membrane, nor did it label the basal body or the periciliary ridge complex (Fig. 6–8, Table I).

As a control, thin sections of albumin embedded retinas were labeled with nonimmune rabbit IgG. No specific labeling of the PE processes, the calycal processes, the CC, or the photoreceptor inner and outer segments occurred (Fig. 9).

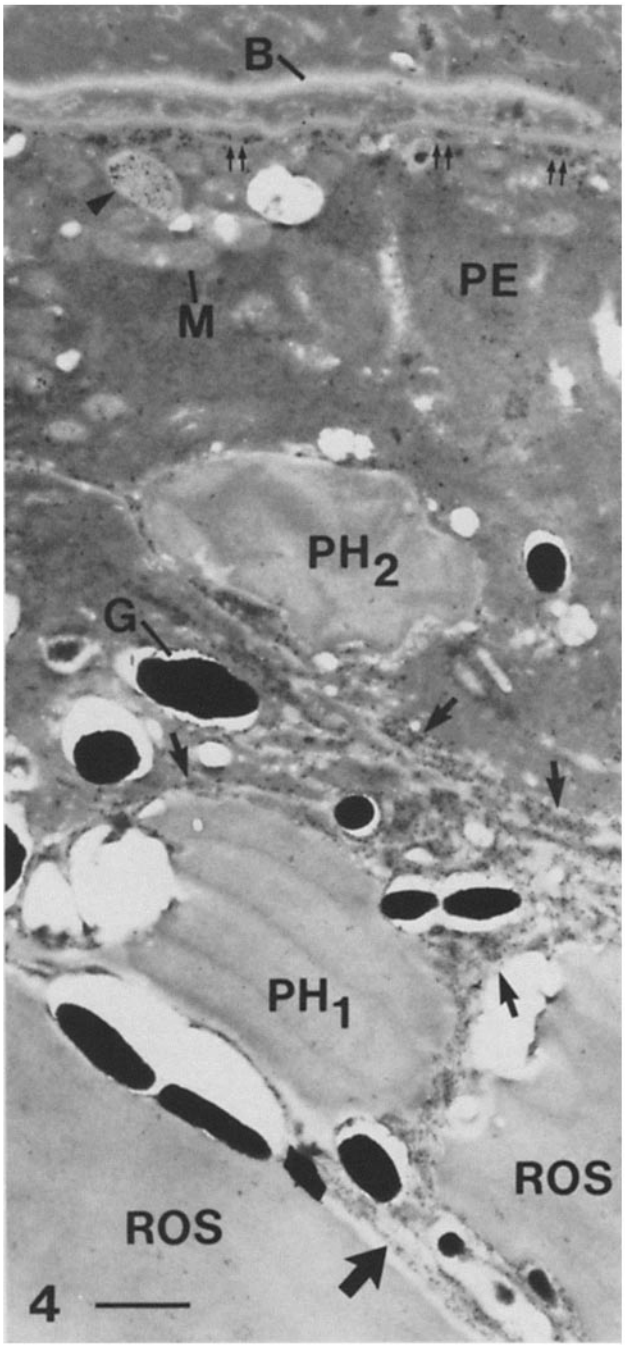

FIGURE 4 Pigment epithelium (*PE*) containing two phagosomes that were shed from the adjacent rod outer segments (*ROS*). Antiactin label is localized to the apical PE (large arrows) and to the PE processes (larger arrow) which interdigitate with the ROS. The phagosome (PH_1) lying adjacent to the tip of an ROS is still surrounded by actin in the apical PE whereas a second phagosome (PH_2) that lies deeper in the PE cell body is no longer surrounded by actin. Label is also observed in the basal PE along Bruch's membrane (small double arrows). This actin localization is being studied further. The oval structure indicated by the arrowhead in the basal PE is filled with a precipitate which is not ferritin. *B*, Bruch's membrane; *G*, pigment granule; *M*, mitochondrion. Bar, 1.0 μm; × 12,480.

DISCUSSION

Actin filaments have previously been identified in the apical PE and PE processes by using heavy meromyosin or myosin subfragment-1 binding to filaments exposed in glycerinated retinas (18–20, 33). In one immunofluorescence study (34) the PE processes in frozen sections of retina became labeled with antiactin antibodies. These actin filaments may mediate the movement of melanin granules in response to changes in the light-dark cycle (18, 20, 33) and they may participate in the phagocytosis of shed packets of OS disks (20). In the present study, when thin sections of albumin embedded retinas were labeled with antiactin antibodies, the apical PE and PE processes were densely labeled (Figs. 3, and 4). These results confirm those of the previous studies, and serve as a positive control for both the specificity and reactivity of the antiactin antibodies used in these experiments. The reactive

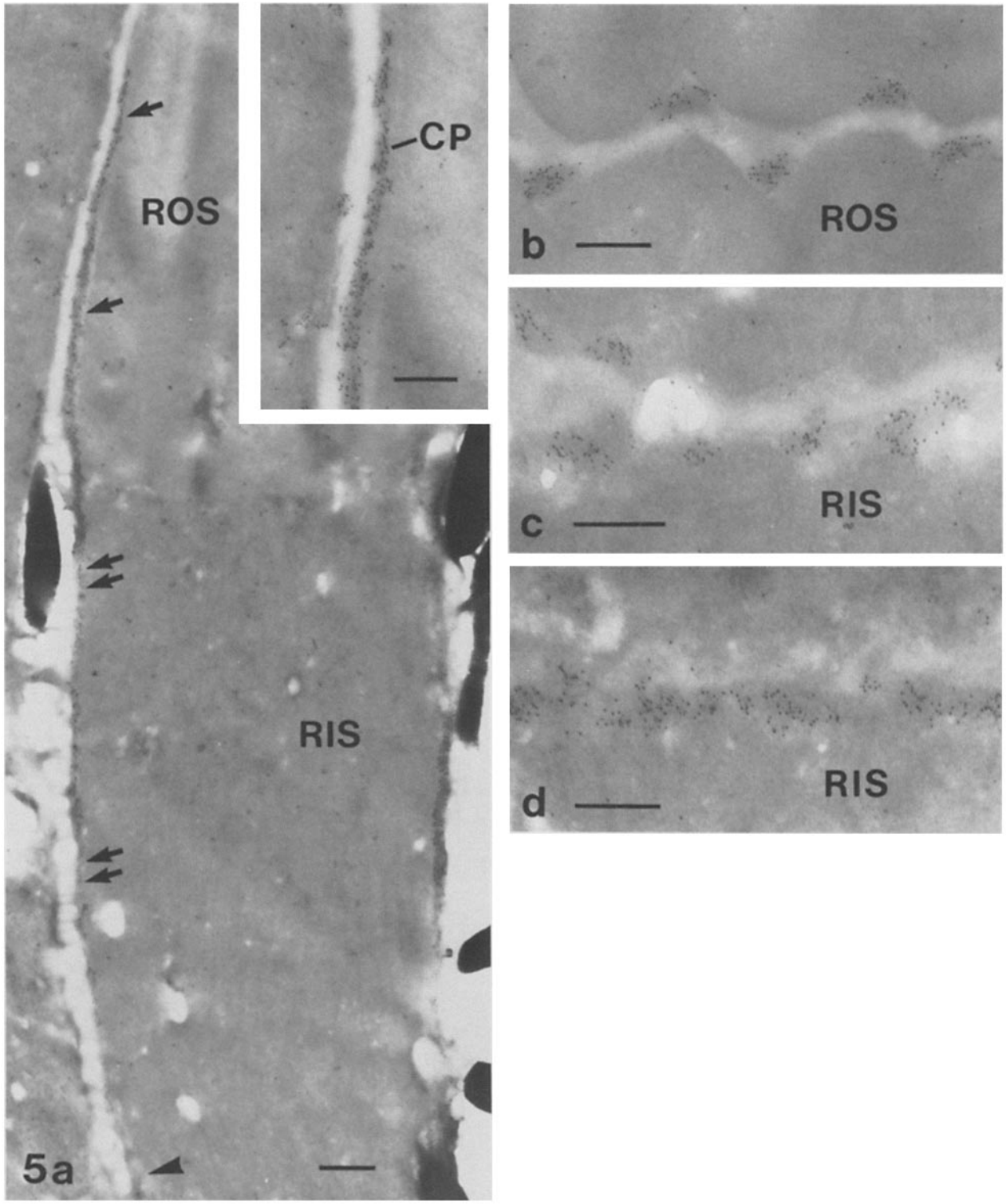

FIGURE 5 Antiactin antibody labeling of actin bundles within calycal processes of rod photoreceptors. (*a*) Photoreceptor showing the basal portion of a rod outer segment (*ROS*) and the ellipsoid (mitochondria rich) region of the rod inner segment (*RIS*). Antiactin densely labels the actin bundles within a calycal process (arrows). This label continues along the bundles as they extend into the RIS, subjacent to the plasma membrane (double arrows). ROS and RIS lack specific antiactin label. The arrowhead indicates the level of the ellipsoid-myoid junction in the RIS. (*Inset*) Higher magnification of the apical end of the calycal process (*CP*). (*b*) Cross-sectioned ROS showing antiactin labeled calycal processes that lie along indentations of the ROS plasma membrane. (*c*) Cross-sectioned upper ellipsoid region of the RIS showing discrete labeled actin bundles that extend from the calycal processes. (*d*) Cross-sectioned lower ellipsoid, near junction with the myoid region of the RIS. Antiactin labels actin which is now more circumferentially distributed beneath the lateral plasma membrane. Bars, 0.5 μm (*a*); 0.25 μm (*b–d*, and *inset*); × 18,480 (a); × 42,500 (*inset*); × 49,300 (*b*); × 60,420 (c); × 56,525 (*d*).

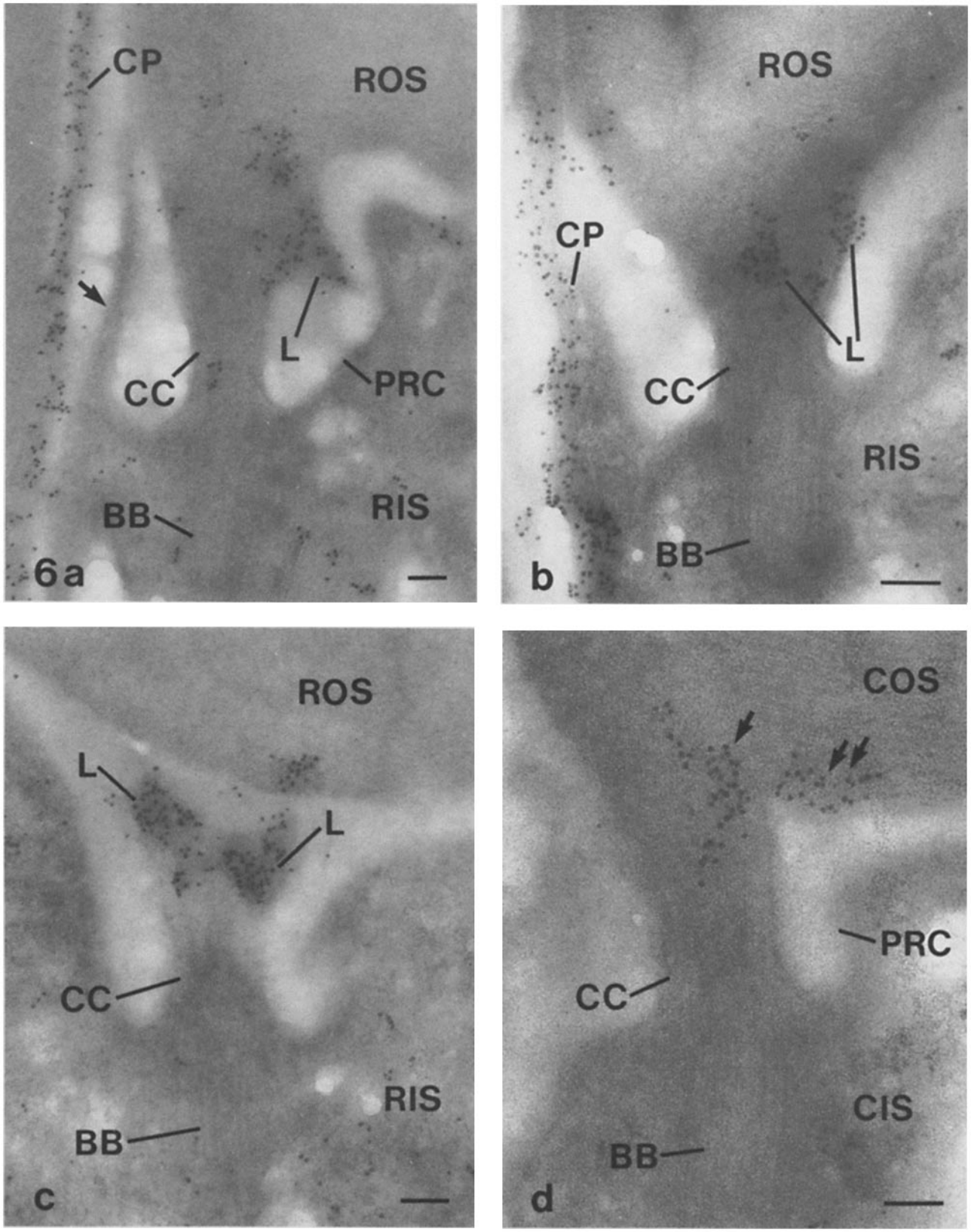

FIGURE 6 Longitudinal sections of photoreceptor connecting cilia (*CC*) labeled with antiactin antibodies. (*a*) This rod CC is heavily labeled by antiactin in the distal portion of the CC and in the interior of a lip-like structure (*L*) that protrudes from the CC just below the basal rod outer segment (*ROS*) disks. Actin in a calycal process (*CP*) of a neighboring photoreceptor is also labeled. A lateral inner segment process adjacent to the CC in this plane of section (arrow) is always observed to be free of antiactin label. This process is a ridge of the periciliary ridge complex (*PRC*). *BB*, basal body; *RIS*, rod inner segment. (*b*) The plane of section in this image appears to be rotated around the CC so that more than one lip (*L*) is observed to be labeled by antiactin. A calycal process (*CP*) is also labeled. (*c*) When the plane of section is rotated approximately 90° from that in Fig. 6*a*, the CC appears to lie in the middle of the cell and two antiactin labeled lips (*L*) are observed. Since this section is slightly oblique to the long axis of the CC, a gap appears between the lips and the ROS. (*d*) Longitudinal section through a cone CC. Antiactin antibodies heavily label the distal portion of the CC (arrow), and in this cone the label extends into the adjacent portions of the most basal outer segment lamellae (double arrows). *CIS*, cone inner segment; *COS*, cone outer segment. Bars, 0.1 μm. × 68,000 (*a*); × 95,040 (*b*); × 84,480 (*c*); × 105,600 (*d*).

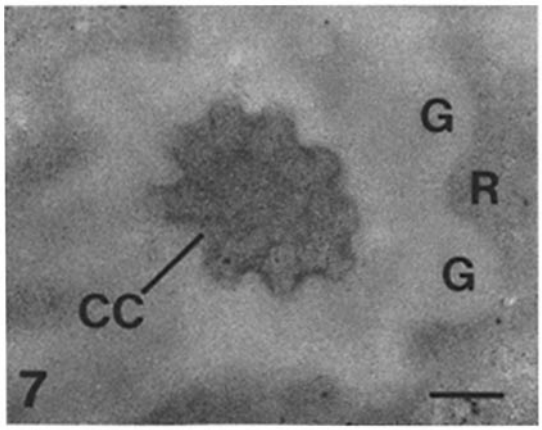

FIGURE 7 Cross-section of a rod connecting cilium (CC) below the actin-rich domain of the distal CC. The interior of the CC, its plasma membrane, and the ridges (*R*) and grooves (*G*) of the surrounding periciliary ridge complex are nearly free of antiactin label. Bar, 0.1 μm; × 96,800.

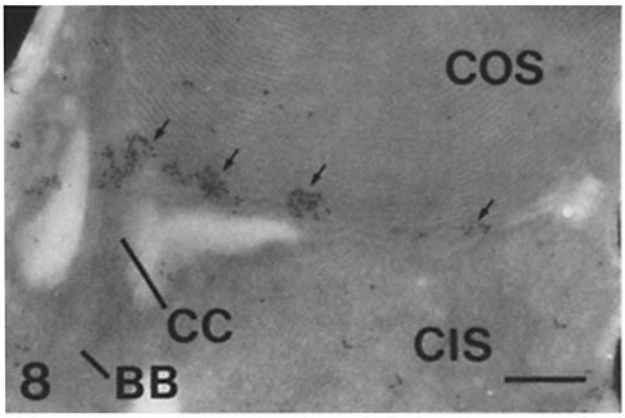

FIGURE 8 Longitudinal section through a cone connecting cilium (*CC*) that joins the inner and outer segments. Antiactin labels the distal portion of the CC. The dense label extends along the basal outer segment lamellae (arrows). The cone inner segment (*CIS*), cone outer segment (*COS*), and basal body (*BB*) are nearly unlabeled. Bar, 0.25 μm; × 42,500.

sites in PE cells also indicate antigen preservation and exposure in these tissue sections.

Adjacent to ROS tips, recently formed phagosomes were situated within antiactin-labeled regions of the apical PE (Fig. 4). As phagosomes moved deeper into the PE cell body the surrounding actin was lost. In recent studies of the phagocytosis of ROS fragments by cultured rat PE cells (26), ROS that attached to the PE cells were shown to be ingested by actin-containing pseudopods that extended from the PE cell surface to surround the ROS. Actin feltworks surrounded newly formed phagosomes, but the feltwork was lost as a phagosome moved deeper into the PE cell body. Thus our in vivo study in frog retinas and the in vitro studies of cultured rat PE cells indicate that a similar sequence of phagocytic events occurs. This result is important for evaluating the use of PE cell cultures as models of PE cell function.

Bundles of actin filaments are also found in the calycal processes of photoreceptors. In teleost cones these filament bundles extend deep into the inner segment, subjacent to the plasma membrane (21). They are believed to take part in a light-induced actomyosin mediated contraction of teleost cones (35). Retinomotor movement also occurs in frog photoreceptors. Our results indicate that actin in the calycal processes of *Rana pipiens* photoreceptors is highly reactive with antiactin antibodies and that the label extends into the depths of the inner segment (Fig. 5) in a distribution similar to that observed in teleost cones. These actin filaments might also function in rod and cone contraction in the frog.

Antiactin did not specifically label photoreceptor outer segments in the present study. However, recent studies of freeze-fractured and deep-etched, rapidly frozen ROS demonstrated filament-like structures on the rims of ROS disks. These filaments connected the rims of adjacent disks and also spanned the deep incisures of amphibian ROS to connect adjacent rims from the same disk (36, 37). Other filaments connected the disk rims to the ROS plasma membrane. The absence of specific antiactin labeling in ROS or COS suggests that these filaments do not contain actin.

At the base of both ROS and COS, in the distal portion of the CC, actin was detected with a high labeling density (Fig. 6, Table I). New disk formation is initiated in this region by an evagination of the CC plasma membrane (11). Actin was also highly concentrated in the cytoplasm of lip-like structures that protrude from the CC just below the basal disks of rods. The plasma membrane of these lips was unlabeled by antiactin antibodies. More than one lip had previously been observed in frog rods using high resolution scanning electron microscopy (7). Lips appear not to be primordial disks (7) and at the present time their function is unknown. Thus actin could be part of a cytoskeleton that maintains lip structure. The concentration of actin in such a small domain in the distal CC and lips indicates that actin may be involved in the final stages of the transport and processing of opsin and other intrinsic membrane proteins that are destined for the newly forming OS disks. As pointed out by Peters et al. (7), the simple lateral diffusion of opsin from the periciliary ridge complex along the CC plasma membrane to the ROS would require a downhill gradient. However, the ROS plasma membrane has a high concentration of opsin. Thus actin in the

TABLE I

Morphometric Quantitation of Ferritin-labeling Densities

Tissue Site	Ferritin grains/square micron ± SE	Tissue site	Ferritin grains/square micron ± SE
Rod lip (11)	1,324 ± 70	Rod outer segment (21)	20 ± 3
Distal rod cilium (5)	1,349 ± 216	Rod inner segment (13)	25 ± 2
Distal cone cilium (5)	1,434 ± 134	Cone outer segment (5)	12 ± 5
Rod calycal process (9)	1,825 ± 141	Cone inner segment (5)	16 ± 7
Cone calycal process (3)	1,778 ± 314	Rod basal body (9)	40 ± 13
Pigment epithelial process (3)	3,012 ± 386	Cone basal body (5)	38 ± 26

Values in parentheses indicate the number of cells counted for each tissue site. Ferritin grain counts for the lips, distal cilia, and inner and outer segments were taken from longitudinally or obliquely cut photoreceptors. Counts for the calycal processes and pigment epithelial processes were taken from longitudinally cut cells only. Counts for the basal bodies were taken from those that were transversely cut as shown in Fig. 6.

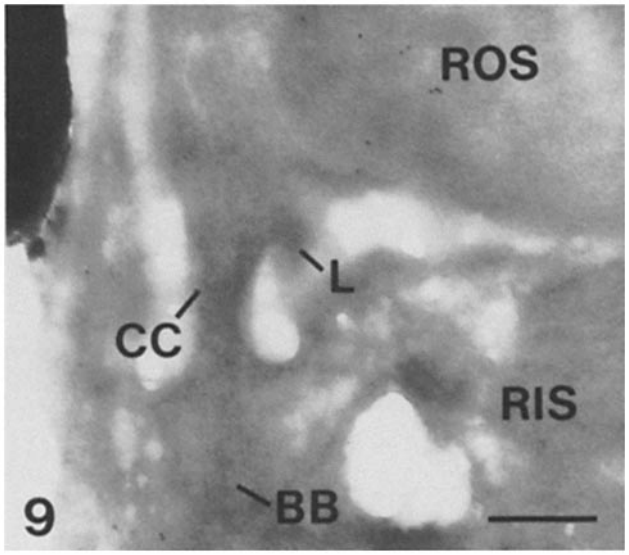

FIGURE 9 Longitudinal section through the periciliary region of a rod photoreceptor reacted with nonimmune IgG as the first stage reagent. Labeling density in this control is negligible. *BB*, basal body; *CC*, connecting cilium; *L*, lip; *RIS*, rod inner segment; *ROS*, rod outer segment. Bar, 0.25 μm; × 56,950.

distal CC and lips may participate in the active transport of opsin to the ROS. Actin in the distal cone CC may function in a similar manner for COS renewal. If so then actin could be the "motive protein" recently suggested to exist in the photoreceptor CC (7).

Antiactin labeling occasionally extended from the CC along the length of the basal disks of ROS and COS (Fig. 8). This result suggests that actin may be involved in the membrane expansion that occurs as new disks are expanding to their final dimensions. A dynamic organization of actin could exist in the leading edge of a growing OS disk, however, a mechanical compression artifact displacing actin into basal disks has not been excluded. We sought light dependent differences in the antiactin labeling of the distal CC, lips and basal OS disks from frog retinas obtained at various times of the light/dark cycle. No differences were detected in these experiments, however the relative rate of new rod and cone disk formation throughout the day has yet to be studied in *Rana pipiens*. If actin is important for the membrane expansion involved with disk formation then the lips seen in rods could act as storage sites for actin.

A possible role for actin in OS disk formation was suggested by results obtained using an in vitro retina culture system. When isolated *Xenopus laevis* retinas were incubated in medium containing cytochalasin B, a complete blockage of open disk formation at the base of ROS was observed (Personal communication, Dr. Joseph C. Besharse, Dept. of Anatomy, Emory University, Atlanta, Georgia). In control retinas, such open basal disks have been used to assay new disk assembly (38).

The localization of actin to the distal portion of the photoreceptor CC, and its possible roles in the vectorial transport of OS membrane proteins and in OS disk formation suggest yet another example of cell membrane motility involving actin. The presence of myosin and an actomyosin contractile mechanism are currently being investigated. It is yet to be determined how a local concentration of actin is restricted to the distal CC and whether or not this actin is maintained in the polymerized or unpolymerized states. Also of interest is how this actin may be associated with the CC plasma membrane. Since photoreceptor OS are renewed throughout life it is possible that a defect in actin-mediated OS disk formation could lead to photoreceptor cell death. Additional studies are in progress to further evaluate the role of actin in OS renewal.

This work was supported in part by United States Public Health Service grants F32 EY05427, EY-03239, -00845, -00046, and -00331, and by the Veteran's Administration.

Received for publication 26 September 1983, and in revised form 6 February 1984.

REFERENCES

1. Young, R. W., and D. Droz. 1968. The renewal of protein in retinal rods and cones. *J. Cell Biol.* 39:169–184.
2. Hall, M. O., D. Bok, and A. D. E. Bacharach. 1969. Biosynthesis and assembly of the rod outer segment membrane system. Formation and fate of visual pigment in the frog retina. *J. Mol. Biol.* 45:397–406.
3. Papermaster, D. S., C. A. Converse, and J. Siu. 1975. Membrane biosynthesis in the frog retina: Opsin transport in the photoreceptor cell. *Biochemistry.* 14:2438–2442.
4. Papermaster, D. S., B. G. Schneider, M. A. Zorn, and J. P. Kraehenbuhl. 1978. Immunocytochemical localization of opsin in the outer segments and Golgi zones of frog photoreceptor cells. *J. Cell Biol.* 77:196–210.
5. Papermaster, D. S., and B. G. Schneider. 1982. Biosynthesis and morphogenesis of outer segment membranes in vertebrate photoreceptor cells. *In* Cell Biology of the Eye. D. McDevitt, editor. Academic Press, NY. 475–531.
6. Besharse, J. C., and K. H. Pfenninger. 1980. Membrane assembly in retinal photoreceptors. I. Freeze fracture analysis of cytoplasmic vesicles in relationship to disc assembly. *J. Cell Biol.* 87:451–463.
7. Peters, K.-R., G. E. Palade, B. G. Schneider, and D. S. Papermaster. 1983. Fine structure of a periciliary ridge complex of frog retinal rod cells revealed by ultrahigh resolution scanning electron microscopy. *J. Cell Biol.* 96:265–276.
8. Papermaster, D. S., C. A. Converse, and M. Zorn. 1976. Biosynthesis and immunochemical characterization of a large protein in frog and cattle rod outer segment membranes. *Exp. Eye Res.* 23:105–115.
9. Papermaster, D. S., B. G. Schneider, M. A. Zorn, and J. P. Kraehenbuhl. 1978. Immunocytochemical localization of a large intrinsic membrane protein to the incisures and margins of frog rod outer segment disks. *J. Cell Biol.* 78:415–425.
10. Papermaster, D. S., P. M. Reilly, and B. G. Schneider. 1982. Cone lamellae and red and green rod outer segment disks contain a large intrinsic membrane protein on their margins: an ultrastructural immunocytochemical study of frog retinas. *Vision Res.* 22:1417–1428.
11. Steinberg, R. H., S. K. Fisher, and D. H. Anderson. 1980. Disc morphogenesis in vertebrate photoreceptors. *J. Comp. Neurol.* 190:501–518.
12. Young, R. W. 1967. The renewal of photoreceptor cell outer segments. *J. Cell Biol.* 33:61–72.
13. Young, R. W., and D. Bok. 1969. Participation of the retinal pigment epithelium in the rod outer segment renewal process. *J. Cell Biol.* 42:392–403.
14. LaVail, M. M. 1976. Rod outer segment disk shedding in rat retina: relationship to cyclic lighting. *Science (Wash. DC).* 194:1071–1074.
15. Basinger, S., R. Hoffman, and M. Matthes. 1976. Photoreceptor shedding is initiated by light in the frog retina. *Science (Wash. DC).* 194:1074–1076.
16. Young, R. W. 1977. The daily rhythm of shedding and degradation of cone outer segment membranes in the lizard retina. *J. Ultrastruct. Res.* 61:172–185.
17. Fisher, S. K., B. A. Pfeffer, and D. H. Anderson. 1983. Both rod and cone disc shedding are related to light onset in the cat. *Invest. Ophthalmol. Visual Sci.* 24:844–856.
18. Murray, R. L., and M. W. Dubin. 1975. The occurrence of actinlike filaments in association with migrating pigment granules in frog retinal pigment epithelium. *J. Cell Biol.* 64:705–710.
19. Burnside, B., and A. Laties. 1976. Actin filaments in apical projections of the primate pigmented epithelial cell. *Invest. Ophthalmol.* 15:570–575.
20. Burnside, M. B. 1976. Possible roles of microtubules and actin filaments in retinal pigment epithelium. *Exp. Eye Res.* 23:257–275.
21. Burnside, B. 1978. Thin (actin) and thick (myosinlike) filaments in cone contraction in the Teleost retina. *J. Cell Biol.* 78:227–246.
22. Besharse, J. C. 1982. The daily light-dark cycle and rhythmic metabolism in the photoreceptor-pigment epithelial complex. *Progress in Retinal Research.* 1:81–124.
23. McLean, J. D., and S. J. Singer. 1970. A general method for the specific staining of intracellular antigens with ferritin-antibody conjugates. *Proc. Natl. Acad. Sci. USA.* 77:7318–7322.
24. Kraehenbuhl, J. P., and J. D. Jamieson. 1974. Localization of intracellular antigens by immunoelectron microscopy. *Int. Rev. Exp. Pathol.* 13:1–53.
25. Schneider, B. G., and D. S. Papermaster. 1983. Immunocytochemistry of retinal membrane protein biosynthesis at the electron microscope level by the albumin embedding technique. *Methods Enzymol.* 96:485–495.
26. Chaitin, M. H., and M. O. Hall. 1983. The distribution of actin in cultured normal and dystrophic rat pigment epithelial cells during the phagocytosis of rod outer segments. *Invest. Ophthalmol. Vis. Sci.* 24:821–831.
27. Jockusch, B. M., K. G. Kelley, R. K. Meyer, and M. M. Burger. 1978. An efficient method to produce specific anti-actin. *Histochemistry.* 55:177–184.
28. Herman, I. M., and T. D. Pollard. 1979. Comparison of purified anti-actin and fluorescent-heavy meromyosin staining patterns in dividing cells. *J. Cell Biol.* 80:509–520.
29. Spudich, J. A., and S. Watt. 1971. The regulation of rabbit skeletal muscle contraction. I. Biochemical studies of the interaction of the tropomyosin-troponin complex with actin and the proteolytic fragments of myosin. *J. Biol. Chem.* 246:4866–4871.
30. Roll, F. J., J. A. Madri, J. Albert, and H. Furthmayr. 1980. Codistribution of collagen

types IV and AB_2 in basement membranes and mesangium of the kidney: An immunoferritin study of ultrathin frozen sections. *J. Cell Biol.* 85:597–616.
31. Heitzmann, H., and F. Richards. 1974. Use of the avidin-biotin complex for specific staining of biological membranes in electron microscopy. *Proc. Natl. Acad. Sci. USA.* 71:3537–3541.
32. Ainsworth, S. K., and M. J. Karnovsky. 1972. Ultrastructural staining method for enhancing the size and electron opacity of ferritin in thin sections. *J. Histochem. Cytochem.* 20:225–229.
33. Burnside, B., R. Adler, and P. O'Connor. 1983. Retinomotor pigment migration in the Teleost retinal pigment epithelium. I. Roles for actin and microtubules in pigment granule transport and cone movement. *Invest. Ophthalmol. Visual Sci.* 24:1–15.
34. Drenckhahn, D., and U. Groschel-Stewart. 1977. Localization of myosin and actin in ocular nonmuscle cells. *Cell Tiss. Res.* 181:493–503.
35. Porrello, K., W. Z. Cande, and B. Burnside. 1983. N-ethylmaleimide-modified subfragment-1 and heavy meromyosin inhibit reactivated contraction in motile models of retinal cones. *J. Cell Biol.* 96:449–454.
36. Usukura, J., and E. Yamada. 1981. Molecular organization of the rod outer segment. A deep etching study with rapid freezing using unfixed frog retina. *Biomed. Res.* 2:177–193.
37. Roof, D. J., and J. E. Heuser. 1982. Surfaces of rod photoreceptor disk membranes: Integral membrane components. *J. Cell Biol.* 95:487–500.
38. Besharse, J. C., J. G. Hollyfield, and M. E. Rayborn. 1977. Turnover of rod photoreceptor outer segments. II. Membrane addition and loss in relationship to light. *J. Cell Biol.* 75:507–527.